Ionomer and Mesomorphic Behavior in a Tail-End, Ionic Mesogen-Containing, Comblike Copolymer Series

Pascal Y. Vuillaume,† Jean-Claude Galin,‡ and C. Geraldine Bazuin*,†

Centre de recherche en sciences et ingéniérie des macromolécules (CERSIM), Département de chimie, Université Laval, Québec, Canada G1K 7P4, and Institut Charles Sadron (ICS), CNRS-ULP, 6 rue Boussingault, 67083 Strasbourg Cedex, France

Received June 7, 2000

ABSTRACT: A series of homologous statistical polymethacrylate comb copolymers with tail-end 4-(dimethylamino)pyridinium ionic groups were synthesized by partial quaternization of high molar mass poly(12-bromododecyl methacrylate). The copolymers of lower ion content are found to be biphasic by differential scanning calorimetry, resembling classical ionomers, with a lower glass transition temperature (T_g) that remains constant up to about 20 mol % ion content before increasing and a higher T_g that increases monotonically with ion content. X-ray analysis indicates the presence of a soft phase with an invariant microstructure for all of the copolymers, whereas the hard-phase microstructure, considered to be a disordered partial bilayer in the ionic homopolymer, is characterized by an increasing long period with decreasing ion content. Models to reconcile the various data are proposed, which show how large amounts of nonionic units can be incorporated into the hard-phase microstructure, with the invariant soft-phase microstructure also rationalized. This copolymer series thus bridges ionomer and mesomorphic polysoap characteristics by the presence of two phases whose relative proportions vary with ion content, both of which possess their own (short-range) microstructure that determines the nature of their evolution with copolymer composition.

Introduction

Both ionomers[1] and liquid crystalline polymers[2] have been extensively studied for many years. In the first, which are generally statistical copolymers with a relatively low proportion of ionic co-units, two-phase behavior is frequently observed due to ionic aggregation in a relatively nonpolar matrix, with consequent reduction in mobility of neighboring nonpolar regions leading to the formation of a second phase of higher glass transition temperature. In the second, which are most commonly composed of flexible and rigid moieties, self-assembly and nanophase separation into specific microstructures (often lamellar for side-chain architecture) frequently occur due to the geometric and chemical dissimilarity of the two moieties. Comblike polymers without mesogenic moieties also generally lead to nanophase-separated morphologies,[3] as do ionic side-chain polyamphiphiles or polysoaps.[4,5] In copolymer form,[6] the latter at lower ion content can be considered as ionomers.

Our group has recently synthesized and studied new tail-end polyamphiphiles of the type poly(ω-pyridinium alkyl methacrylate)s with various 4-substituted pyridinium bromide groups and spacer lengths.[5] They generally present an amorphous, lamellar-like morphology, with a single, well-defined glass transition whose value depends markedly on the spacer length and nature (rigidity, volume) of the pyridinium moiety. As a corollary to those homopolyamphiphiles, this paper describes a series of copolyamphiphiles prepared by partial quaternization of a nonionic precursor polymer, a poly(ω-bromoalkyl methacrylate), by one of the pyridine moieties used for the homopolymer series, namely (dimethylamino)pyridine (DMAP). This provides a unique set of copolymers combining several aspects of the above-mentioned classes of materials. In particular, they are comb copolymers possessing two different types of long side chains of identical spacer length, one nonionic and the other ionic, where the terminal ionic moiety resembles a (short) thermotropic mesogen. Their general structure is shown in Scheme 1, noting that charge delocalization is possible over the DMAP cation.

Scheme 1

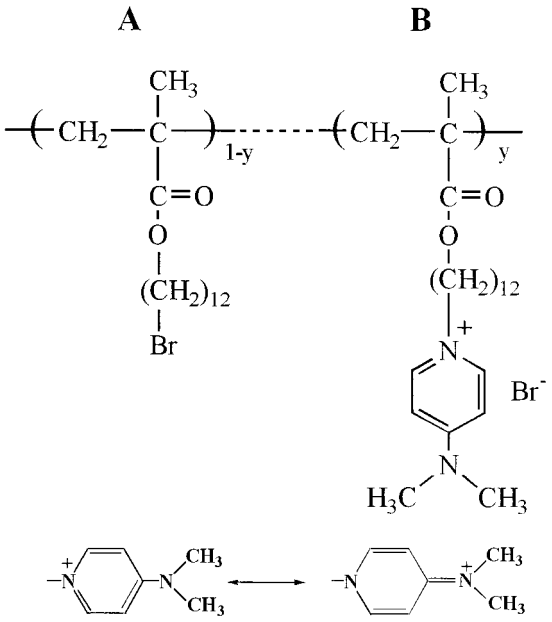

These copolymers may thus be expected to form a bridge between ionomers on one hand and tail-end amphiphilic homopolymers (side-chain liquid crystalline or mesomorphic homopolymers) on the other. They are complementary to a rather small number of other ionic

* To whom correspondence should be addressed.
† Université Laval.
‡ Institut Charles Sadron.

10.1021/ma001000m CCC: $20.00 © 2001 American Chemical Society
Published on Web 01/17/2001

copolymers and ionomers with side-chain liquid crystalline or mesomorphic character that have been reported in the literature.[6−10] In these studies, the ionic group is usually located near the polymer backbone and is often distinct from a classic mesogenic group, and its content is limited to low values in several cases. An investigation of ionomers with ionic groups located at the end of long side chains[11] should also be mentioned for comparison.

In the following, we will describe the thermal and structural properties of the copolymers, in addition to their synthesis, and relate their behavior to ionomer and mesomorphic characteristics. The copolymers will be denoted as AB-*y*, where A and B refer to the nonionic and ionic units, respectively. F_i and W_i denote the molar and weight fractions, respectively, of component *i* (A or B) in the copolymers, with *y* equal to $100F_B$. Thus, AB-17 is a copolymer containing 0.17 molar fraction of B units (17 mol % ion content).

Experimental Part

Materials. All reagents were obtained from Aldrich. Tetrahydrofuran (THF) was distilled over a disodium benzophenone complex and dimethylformamide (DMF), toluene, and triethylamine over calcium hydride. Acetonitrile was dried over molecular sieves (4 Å). Hexane, ethyl acetate, methanol, 4-(dimethylamino)pyridine (DMAP), 12-bromododecanol, and methacrylic anhydride, all of the best reagent grades available, were used as received. 2,2′-Azobis(isobutyronitrile) (AIBN) was recrystallized from toluene. Column chromatography was performed using silica gel [Merck, Kieselgel 60 (70−230 mesh)]. Thin-layer chromatography (TLC) was carried out on precoated silica gel plates (Merck, F-254).

Techniques of Analysis. NMR spectra were recorded at ambient temperature with a 200 MHz Bruker spectrometer. Chemical shifts, δ, are given in ppm with respect to the solvent residual resonances, fixed at 7.27 ppm for $CDCl_3$. Elemental analysis was performed in-house (ICS).

Differential scanning calorimetry (DSC) investigations were carried out using a Perkin-Elmer DSC-7 calorimeter, calibrated with indium (T_m = 156.6 °C, ΔC_p = 28.5 J g^{-1} $°C^{-1}$) and, in some cases, mercury (T_m = −38.8 °C) to validate the low-temperature transitions. The sample chamber was flushed with He or N_2. Heating scans were performed at 20 °C/min after quenching (nominally −200 °C/min), never exceeding 160 °C (samples confirmed to be stable to at least this temperature by thermogravimetric measurements), on 10−20 mg of samples dried in vacuo for 6 days at 60 °C or 2 days at 80 °C prior to sealing in aluminum pans. The glass transition temperatures (T_g) were determined by the midpoint of the heat capacity jump and verified by the maximum of the peaks in the first derivatives of the scans. For the copolymers with a double T_g, the intermediate minimum in the first-derivative curves served as a check on the location of the estimated intermediate baseline (arbitrarily given a slope similar to those of the baselines before and after the double T_g). The data obtained are based on at least five scans involving a minimum of two different capsules per sample. It was verified that more rigorous drying conditions (2 days at 100 °C in vacuo for samples placed in pans with previously pierced covers) and slow cooling (−20 °C min^{-1}) did not affect the results.

Polarizing optical microscopy (POM) observations of the samples were made using a Zeiss Axioskop equipped with a Leica (UT40/0.34) objective. The temperature was regulated with a Mettler FP5 temperature controller and Mettler FP52 hot stage.

Two sets of X-ray diffraction data were obtained on dried samples placed in sealed Lindemann capillaries (Charles Supper) of 1.5 mm i.d. for $y \geq 27$, and in the form of 1 mm thick films (molded between two Teflon-lined aluminum plates pressed together via a screw-down mechanism at 120 °C in vacuo for about 5 h) for the other samples. The first set covered 2θ angles between 1.1° and 40°, using nickel-filtered Cu Kα radiation (1.542 Å) produced by a Rigaku rotating anode X-ray generator (Rotaflex RU-200BH), operated at 55 kV and 190 mA, with collimation effected by a Soller slit and a 1 mm pinhole. A scintillation counter (SC-30) coupled to a pulse-height analyzer was used as detector, with a sample-to-detector distance of 37.2 cm. The profiles obtained were left untreated, but it was verified that there were no specific features in the background that could obscure the results.

The second set of data covered the small-angle region, using a Bruker diffractometer equipped with a sealed-tube Cu anode operated at 40 kV and 40 mA and a two-dimensional position-sensitive wire detector; collimation was effected by a graphite monochromator and a 0.8 mm pinhole. The sample-to-detector distance was fixed at 9 cm for samples with $y \geq 58$ and at 20 cm for the others, using a homemade beam stop, which was off-centered for the latter configuration in order to cover a 2θ range between 0.7° and 5°. After subtraction of the capillary background for the copolymers of high mesogen content and of air scattering for the other copolymers, the appropriate 2D range was integrated to obtain intensity as a function of 2θ.

Molecular lengths (*l*) for the A and B units in their lowest energy conformation with *all-trans*-methylene units were estimated from Hyperchem 3 software (Hypercube Inc.). This length corresponds to the distance from the outermost hydrogen of the methyl group on the polymer backbone to the terminal atom of the side chain (including van der Waals radius at the extremities, but not including the Br^- ion in the B unit).

Synthesis of Monomer. *12-Bromododecyl Methacrylate* (*A*). To a solution of 5 g (18.8 mmol) of 12-bromododecanol, 3.9 mL (28.3 mmol) of triethylamine and 0.230 g (1.9 mmol) of 4-(dimethylamino)pyridine in 50 mL of THF previously cooled to 0 °C were added dropwise under a nitrogen atmosphere and while stirring 4.2 mL (28.3 mmol) of methacrylic anhydride. The solution was stirred overnight at room temperature, then concentrated to half of its volume by rotary evaporation, and diluted with 150 mL of an aqueous solution of NaCl. The monomer was extracted with hexane, and the organic phase washed three times with an aqueous solution of Na_2CO_3. Hexane was exhaustively removed by rotary evaporation, and the crude product was purified by column chromatography [eluent: hexane/ethyl acetate (90/10 v/v)]. Yield: 3.1 g (62%) of a yellow oil. Anal. Calcd for $C_{16}H_{29}O_2Br$: C, 57.66; H, 8.77; O, 9.60; Br, 23.97. Found: C, 58.07; H, 9.23; O, 9.17; Br, 23.27. ^1H NMR (200 MHz, $CDCl_3$): δ = 6.09 and 5.54 [2s, 2H, CH_2═C]; 4.13 [t, 2H, CH_2−O]; 3.40 [t, 2H, CH_2−Br]; 1.94 [s, 3H, C═C(CH_3)]; 1.85 [m, 2H, CH_2−C−Br]; 1.67 [m, 2H, CH_2−C−O]; 1.15−1.45 [m, 16H, C−$(CH_2)_8$−C].

Polymerization and Quaternization. The reactions were performed in a double-walled reactor fitted with a magnetic stirrer and connected to an external Lauda thermostat (temperature monitored to ±0.1 °C). The system containing the solvent and all the reagents was degassed at room temperature by three successive vacuum-argon sweeping cycles. The reactions were then performed at constant temperature for a given time under slightly positive argon pressure.

Poly(*12-bromododecyl methacrylate*) (*An*). Free radical polymerization was performed in a homogeneous ethyl acetate solution under the following experimental conditions: [A] = 1.3 mol L^{-1}; [AIBN] = 6.5 × 10^{-3} mol L^{-1}; 60 °C; 17 h. The resulting polymer was recovered by precipitation into methanol and dried in vacuo at 40 °C. Yield: 78%; $M_w = 1.3 \times 10^6$ from light scattering (Chromatix CMX 100) in THF solution (d*n*/d*c* = 0.082 mL g^{-1} at λ = 632 nm).

Quaternized Copolymers (*AB-y*). Reaction of the precursor polymer, An, with calculated amounts of DMAP was performed in a 10−15 wt % homogeneous DMF/toluene (50/50 v/v) solution for 48 h at 60 °C while stirring. The copolymers were recovered by precipitation into diethyl ether, thoroughly washed with diethyl ether, and dried at 40 °C in vacuo. Elemental analysis (C, H, N, Br) lead to self-consistent compositional data. The number *y* in AB-*y* thus represents the

Scheme 2

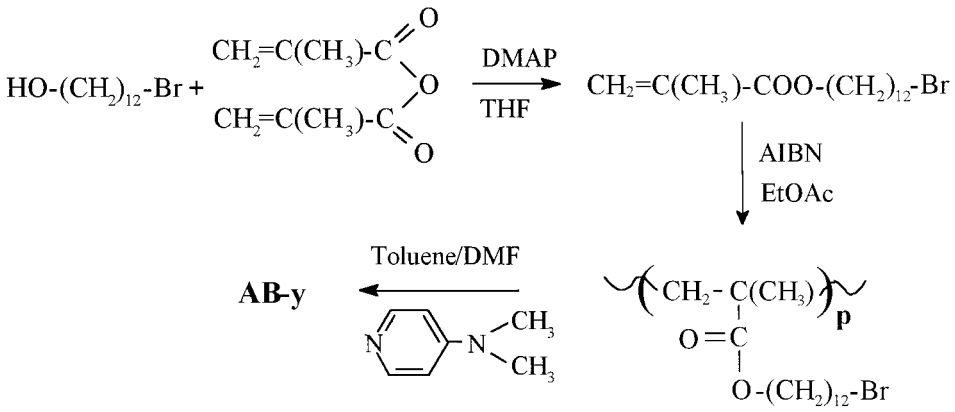

mole percent quaternization determined from the N content. For one copolymer (AB-17), the Br^- ion content was also determined by potentiometry in a toluene/methanol/acetic acid (5v/40v/4v) mixed solvent using 0.01 N aqueous $AgNO_3$ as titrating agent. This gave a mole fraction of Br^-, $F_B(Br^-) = 0.168$, in excellent agreement with $F_B(N) = 0.174$ based on the N content.

It was noted that, whereas the copolymer solutions remained apparently homogeneous after completion of the quaternization reaction, the copolymers with higher quaternization degrees were difficult, if not impossible, to redissolve following recovery and drying. This was also observed for the homopolymer, Bn, and similar quaternized homopolymers.[5] Since the method of synthesis of the copolymers should preclude any cross-linking, this lack of solubility is presumably related to the particular amphiphilic character of the pyridinium tail-end polymers, combined with the effects of high molar mass, as previously postulated for the homopolymers.[5]

Poly(12-methacryloyloxydodecyl-4-(dimethylamino)pyridinium bromide) (*Bn*). To ensure quantitative quaternization, the homopolymer Bn was synthesized by free radical polymerization of the corresponding monomer, as described previously.[5]

Results

Copolymer Synthesis. The general strategy of the copolymer synthesis, shown in Scheme 2, is based on the controlled functionalization of a high molar mass polymer precursor, An, to obtain a series of homologous copolymers, AB-*y*, of different compositions but identical chain length, similar unit distribution, and similar high compositional homogeneity. The successive steps, detailed in the Experimental Section, will be commented on briefly in what follows.

In the first step, esterification of 12-bromododecanol by methacrylic anhydride catalyzed by DMAP gave pure methacrylate A in fair yield (~60%) and was more successful than acylation using methacryloyl chloride. It should be emphasized that the monomer thus obtained is completely free from any dimethacrylate species. By contrast, in the route described in a previous publication,[5] where the monomer was prepared through an SN_2 substitution between an excess of 1,12-dibromododecane and cesium methacrylate, contamination by minute amounts of dimethacrylate—and hence light cross-linking leading to incompletely soluble precursor polymer (An) that could complicate subsequent quaternization—cannot be rigorously excluded.

In the second step, free radical polymerization of monomer A in homogeneous ethyl acetate solution leads to high molar mass chains, $DP_w \sim 3.9 \times 10^3$, with a good yield of 78% (see Experimental Section).

In the final step, quaternization of the precursor polymer, An, by DMAP was performed in solution in the binary solvent, toluene/dimethylformamide (50/50 v/v), where both the precursor and functionalized copolymers are completely soluble. The degree of quaternization is determined by the initial ratio $r = [DMAP]_0/[A]_0$. In the experimental conditions used (see Experimental Part), quaternization, favored by the presence of a highly dipolar aprotic solvent like DMF,[12] is quantitative even for the copolymer of highest *r* value synthesized: $F_B = 0.58$ for $r = 0.58$. Moreover, no chain scission is expected to have occurred during the reaction given that it was performed at a moderate temperature of 60 °C under an argon atmosphere.

Although a detailed analysis of the unit distribution along the copolymer chain, AB-*y*, and of the compositional homogeneity is beyond the scope of this work, some general aspects should be discussed. According to literature data,[13,14] kinetics of quaternization of chlorinated polymers [usually poly(*p*-chloromethylstyrene)] by tertiary amines (in one case, a long chain alkylamine[13]) in homogeneous solution in polar solvents generally show only fairly weak deviations from ideal behavior, at least for moderate conversions (≤50%): one rate constant throughout the reaction and no significant neighboring group effects,[15] despite potential steric effects, which are otherwise a major factor in quaternization reactions of amines[12] [in particular, of polyamines such as poly(vinylpyridines)[15]]. In our system, because of the very efficient decoupling of the reaction site from the polymer backbone by the long alkyl spacer, deviations from ideal behavior should be even more negligible than in the systems just cited. Under these conditions, the unit distribution is Bernoullian and may be expressed in terms of the mole fraction of B units centered in the various triads and of the average length of B blocks, $\bar{l}_B$:

$$F(\mathrm{ABA}) = (1 - F_B)^2 \tag{1}$$

$$F(\mathrm{ABB} + \mathrm{BBA}) = 2(1 - F_B)F_B \tag{2}$$

$$F(\mathrm{BBB}) = F_B^{\,2} \tag{3}$$

$$\bar{l}_B = \frac{1}{1 - F_B} \tag{4}$$

The mole fraction of nonisolated B units is already significant even for low B content: $F(\mathrm{ABB} + \mathrm{BBB}) = 0.19$ for $F_B = 0.10$. With the same kinetic assumption,

Table 1. DSC Data for the Various Copolymers and the Corresponding Homopolymers[a]

polymer	W_B	T_g^S (°C)	ΔC_p^S (J g^{-1} °C^{-1})	T_g^H (°C)	ΔC_p^H (J g^{-1}°C^{-1})	W^S	W_B^S	W_B^H
Bn	1			76	0.33			
AB-58	0.65			49	0.24	0		0.65
AB-27	0.34	−37	0.08	16	0.16	0.33	0.06	0.49
AB-17	0.22	−50	0.16	1	0.07	0.49	0	0.43
AB-9	0.12	−51	0.23	−6	0.03	0.70	0	0.40
An	0	−52	0.33					

[a] For the biphasic copolymers, the ΔC_p^S and ΔC_p^H data are the primary values normalized to 1 g of copolymer.

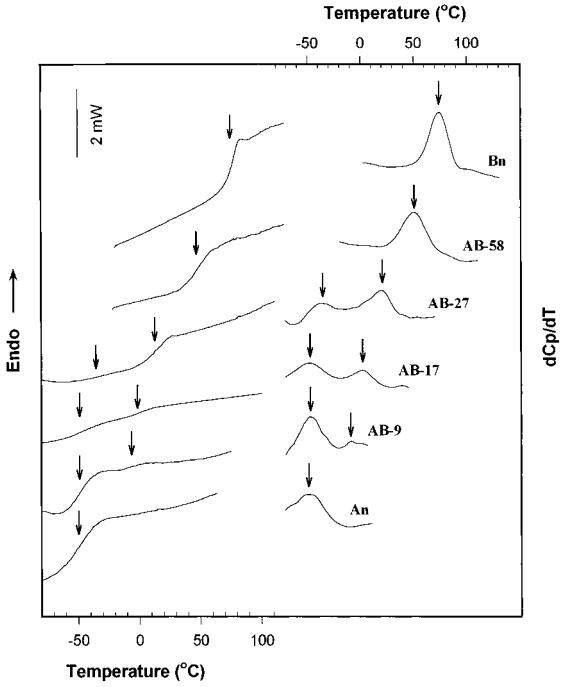

Figure 1. DSC thermograms of the polymers studied and their corresponding first derivatives, with the T_g's specified by arrows.

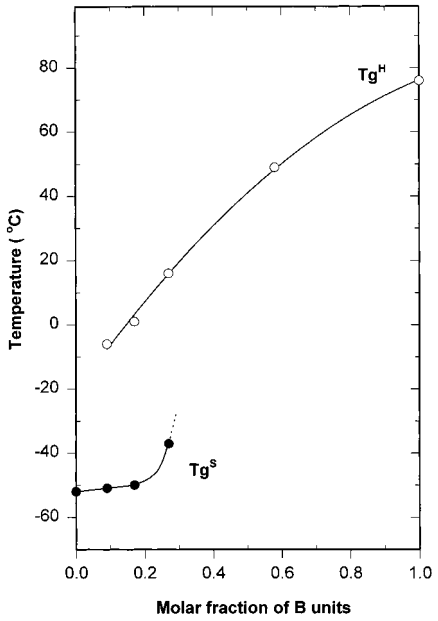

Figure 2. Glass transition temperatures of the soft (T_g^S) and hard (T_g^H) phases as a function of ion content for the AB-*y* copolymers and corresponding homopolymers.

the mean-square standard deviation for the composition, σ^2, may be readily approximated by[16]

$$\sigma^2 = \frac{F_B - F_B^2}{\overline{DP}_n} \tag{5}$$

Given the high molecular weight of the polymer precursor, eq 5 indicates that the copolymers have very good compositional homogeneity.

Thermal Characterization. The DSC thermograms for the copolymers and homopolymers studied, and their corresponding first derivatives, are given in Figure 1, with the T_g's and heat capacity increments (ΔC_p) listed in Table 1. The copolymer of highest ion content (F_B = 0.58) displays a single, well-defined glass transition, as do the homopolymers, whereas the other three copolymers (F_B = 0.09, 0.17, and 0.27) show two glass transitions, which are particularly evident in the derivative curves, at "low" and "high" temperature. The variation of the T_g's as a function of composition is illustrated in Figure 2. The low T_g increases in temperature very little, if at all, up to about 20 mol % ion content, compared to that of the homopolymer An, and then appears to increase rapidly before no longer being detectable somewhere below 58 mol % ion content. The high T_g is observed in all of the copolymers studied, including AB-9, and increases with ion content toward the value for the homopolymer Bn. The intensities of the low and high T_g's, measured by the corresponding heat capacity increments, ΔC_p, decrease and increase, respectively, with increase in ion content (Table 1).

These features are characteristic of a biphasic material and may readily be explained by the Eisenberg−Hird−Moore (EHM) "multiplet-cluster" concept developed for classical ionomers;[1,17] namely, the coexistence of an ion-poor "soft" phase of low T_g (T_g^S) and of an ion-rich "hard" phase of high T_g (T_g^H), whose proportion decreases and increases, respectively, with increase in B content. [The soft and hard phases are also frequently referred to, in the ionomer literature, as the "matrix phase" and the "cluster phase", respectively. Ionic groups or ionic aggregates called multiplets may be dispersed in the soft or matrix phase. The hard or cluster phase is essentially composed of complex aggregates of multiplets along with a considerable proportion of nonionic material whose mobility is significantly reduced, thus leading to a higher T_g than the soft or matrix phase.[1]] It is notable that the two T_g's are DSC-detectable in our materials, as for only a minority of other ionomers; most often, they are detected instead by dynamic mechanical methods.[1]

The constancy of T_g^S up to $F_B \sim 0.2$ [$T_g^S \sim T_g$(An)] indicates that the soft phase is essentially a pure An phase devoid of B units in this ion content range. This contrasts with the behavior of most statistical ionomers,[1] including styrene ionomers with the ionic group at the end of a long alkyl spacer, where low but significant amounts of ionic units are present in the soft phase.[11] A similar purity of the matrix is observed in segmented ionenes and zwitterionomers[18] and is also generally expected for block copolymers.

For AB-27, the increase in T_g^S may suggest that a certain proportion of B units are now incorporated into the soft phase, as generally observed in ionomers. Another explanation for the T_g^S increase may be the reduction in mobility caused by the soft phase being embedded as a minority phase of reduced size (consistent with the low ΔC_p) within what is now a hard-phase matrix (high ΔC_p), accompanied by strong interconnectivity of the two phases through common chains crossing the interfaces.[19,20] In other words, the soft phase is still sufficiently large to be detected by DSC as a separate phase but small enough that the "hard-wall" effect of the surrounding hard phase to which it is strongly connected (creating an "interphase" of reduced mobility[17,20]) is pronounced.

The lack of a DSC-detectable soft phase for AB-58 may be compared with the behavior of a series of statistical biphasic *n*-butyl acrylate zwitterionomers[21] for which a similar feature occurs near $F_B = 0.5$. The apparent monophase (hard phase) in AB-58 must obviously contain a high proportion of A units, accounting at least in part for the decrease of its T_g compared to that of Bn. The continued decrease of T_g^H with increase in overall A-unit content in the biphasic copolymers suggests that the proportion of A units in the hard phase also increases as the overall A content increases and/or that the decreasing size of the hard-phase regions results in increasing influence of the interconnected soft phase on their mobility.

The DSC data can be used to analyze semiquantitatively the biphasic structure in terms of the relative importance of the soft and hard phases (weight fractions W^S and W^H, respectively) and their internal composition (weight fraction W_i^j with i = A or B and j = H or S), as often done for biphasic materials such as segmented copolymers and ionomers with two DSC-detectable T_g's.[18,22] For the two copolymers of lowest ion content ($F_B = 0.09$ and 0.17), the apparent purity of the soft phase indicates that $W_A^S = 1$. Straightforward calculations, involving only the experimental values of the heat capacity increment, ΔC_p^S, of the fairly well-defined low-temperature glass transition and a simple mass balance, lead to the following relations:

$$W^S = \Delta C_p{}^S/\Delta C_p{}^{An} \quad \text{with } W^H = 1 - W^S \qquad (6)$$

$$W_B{}^H = W_B/(1 - W^S) \quad \text{with } W_A{}^H = 1 - W_B{}^H \qquad (7)$$

where ΔC_p^{An} is the heat capacity increment at the T_g of the homopolymer An. The resulting values for AB-9 and AB-17 are given in Table 1.

It is noted that eq 6 implicitly assumes that the intrinsic heat capacity increment at T_g^S (ΔC_p^S normalized to 1 g of the soft phase) is identical to ΔC_p^{An}, in other words, that ΔC_p^S decreases in the copolymers only because of the loss of a fraction of the A units to the hard phase. In fact, the interconnectivity of the domain structure and the resulting reduction of chain mobility in the matrix due to the hard domains behaving as physical cross-links may also lower ΔC_p^S, the more so the higher the B content.[19,23,24] Thus, the W^S and W_B^H values given in Table 1 could be slightly underestimated, in particular for AB-17, which is near the limit that has been estimated (average molar mass between cross-links of ca. 2000 g/mol[23]) below which the interconnectivity effect is insignificant.

For the biphasic copolymer of highest ion content, AB-27, the soft phase with its higher T_g might include some ionic units (implying $W_A^S < 1$) and certainly would be subject to the effects of interconnectivity on ΔC_p^S, so that the previous calculations are no longer valid. Moreover, again because of the interconnectivity of the domains, the composition of the soft and hard phases cannot be calculated from any T_g−composition equations, which all suppose that the phases are independent. In an alternative, very empirical approach, a rough but reasonable estimate of the structural parameters may be obtained by plotting the variations of W^H and W_B^H with W_B for the two copolymers of lower ion content and graphically extrapolating to higher W_B [knowing that W^H and W_B^H must increase monotonically with W_B ($W^H = 1$ for $W_B = 0.65$) and ensuring that mass balance is respected by the extrapolated values]. The results of this extrapolated approximation for AB-27 are given in Table 1. Interestingly, it indicates that there are insignificant amounts of ionic B units in the soft phase of even this copolymer.

Although the specific numerical results of the above calculations must be taken with caution, the tendencies observed are certainly reasonable and consistent with the qualitative observations described earlier. It may be noted that the calculations indicate that the segregation rate of A units, SR, which measures the fraction of A units located in the soft phase of the biphasic copolymers ($SR = W_A^S W^S/W_A$; SR = 1 for quantitative segregation), appears as a decreasing function of ion content: SR = 0.79, 0.63, and 0.47 for AB-9, AB-17, and AB-27, respectively. The calculations also suggest that, although the ionic B units are located (almost) exclusively in the hard phase, the A units nevertheless predominate in this phase, with the molar ratio F_A^H/F_B^H appearing as a decreasing function of ion content at 2.0, 1.8, and 1.4 for AB-9, AB-17, and AB-27, respectively.

Structural Characterization. When observed through the polarizing optical microscope, all of the copolymers studied, as well as the two homopolymers, display an ill-defined white birefringence, which is indicative of the existence of some order in the materials. It tends to decrease in intensity but to persist to higher temperatures, with decrease in pyridinium content, being no longer observable by about 100 °C for Bn and AB-58 and by about 150, 170, and 200 °C for F_B = 0.27, 0.17, and 0.09, respectively; birefringence persists to at least 200 °C for An.

In view of the POM observations, X-ray studies were undertaken, and Figure 3 shows the ambient temperature profiles obtained. A common feature of all profiles is the diffuse band at wide angles, centered near 2θ = 19.5°, that reflects the average lateral distance (~4.5 Å) between disordered side chains. The absence of sharp peaks in this region indicates the absence of any crystallinity.

At smaller angles, the profiles vary with ion content. That for the fully quaternized homopolymer, Bn, shows two weak diffraction peaks at about 2.5° and 5.3° (2θ). Their reciprocal distances are approximately in the ratio 1:2, and the derived Bragg spacing, d, is 35 Å, compared to a calculated molecular length, l, of 28 Å for the fully extended B unit. As discussed elsewhere for Bn and similar polyamphiphiles,[5] this profile is consistent with lamellar ordering in the form of a partial bilayer over rather short correlation distances.

The profile of the nonionic homopolymer, An, also shows two small-angle peaks, which are still weaker,

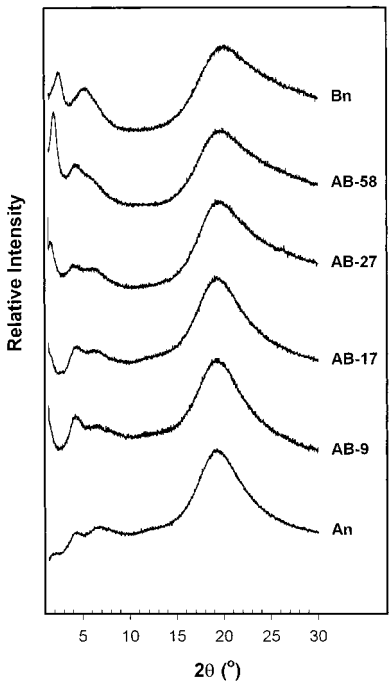

Figure 3. Ambient temperature X-ray diffractograms of the AB-*y* copolymers and corresponding homopolymers.

at 4.3° and 6.5° (2θ). These two peaks are visible in the profiles of all of the copolymers studied, and their position appears invariant within the precision of the measurements. It can be concluded that they reflect an essentially pure or unmodified An phase in the copolymers and that this phase is structured, albeit imperfectly or over short correlation lengths considering the weakness of the reflections. The first peak at $2\theta = 4.3°$ indicates a Bragg spacing, d, of 21 Å compared to a calculated molecular length, l, of 23 Å for the fully extended A unit. These peaks possibly reflect a lamellar organization, as is considered to be the case for amorphous long-chain *n*-alkyl polymethacrylates.[3] If so, the observation that their reciprocal distances are in a ratio of about 2:3 would suggest that they correspond to second- and third-order reflections of an essentially bilayer arrangement. (Indeed, there appears to be a hint of what is perhaps a very weak first-order peak near $2\theta = 2.2°$, but this was not verified by the small-angle data in Figure 4.) Other microstructures are not excluded.

For AB-58, the two peaks in the Bn profile move to smaller angles, with the second-order peak appearing approximately coincidental with the (invariant) An reflection at $2\theta = 4.3°$. The latter is deduced from the fact that the intensity of the peak at this position is greater than that of the An peak near $2\theta = 6.5°$ (in the form of a shoulder in this copolymer), contrary to what is observed for An and the other copolymers. It is also notable that the intensity of the first-order Bn peak is now significantly greater than that of the second-order reflection, in contrast to the Bn homopolymer and other similar polysoaps.[5] In AB-27, only the first-order Bn peak seems to be present, and it has moved to still smaller angles. This peak is much reduced in intensity in AB-17 and is barely if at all visible in AB-9 but appears to undergo little further change in position.

To verify the variation in position of the smallest-angle Bn peak with composition, a series of X-ray experiments optimized for the small-angle region were performed, and the profiles obtained are shown in Figure 4. Here, it is unambiguous that the Bn peak is indeed present in all of the copolymers, and its position decreases with decrease in B content. The corresponding Bragg spacings or long periods, d, are plotted as a function of mole percent B content in Figure 5. The variation in the data appears linear (within the limits

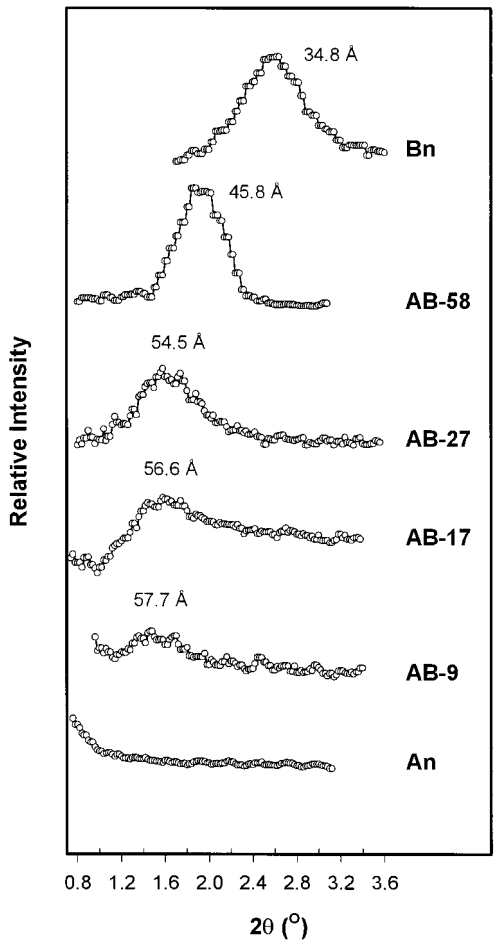

Figure 4. Small-angle X-ray profiles at ambient temperature of the AB-*y* copolymers and corresponding homopolymers. The numbers given are the Bragg spacings (d) calculated from the peak maxima.

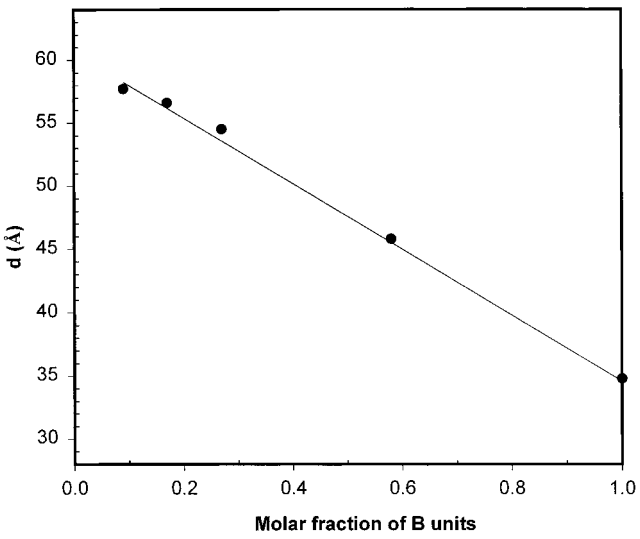

Figure 5. Bragg spacings (from Figure 4) as a function of ion content, with a least-squares fit shown by the solid line.

of the small number of points available) with a slope of 0.27 Å/mol %, although it is also possible to view d as tending toward a maximum of about 58 Å at low B content.

In summary, the diffraction profiles for the copolymers appear to be a superposition of that for the brominated homopolymer (An pattern), which is invariant, and that related to the pyridinium homopolymer (Bn pattern), which moves to lower angles and loses the second-order reflection as the pyridinium content decreases. In light of the two-phase morphology of the copolymers, as revealed by the DSC analysis, the two patterns can be associated with the soft and hard phases, respectively, of the copolymers. The invariance of the An pattern indicates that the B units are essentially excluded from the An phase, which remains present up to high B content (at least 58%) at the detection level of the X-ray experiments. In contrast, the evolution of the Bn pattern indicates that A units are somehow incorporated into the hard-phase microstructure.

Discussion

We will first consider how the evolution in the hard-phase microstructure with increasing A content can be accounted for and propose two possible models, then we will rationalize the constancy of the soft-phase microstructure, and, finally, we will discuss the consistency between the thermal behavior and the proposed models. As mentioned above and analyzed previously,[5] the microstructure of the homopolymer, Bn, is most likely lamellar in nature, albeit with a short correlation length. A reasonable packing arrangement proposed in ref 5 is shown schematically in Figures 6a and 7a. (Other packing arrangements are not excluded, such as a different degree of interpenetration of the mesogens, an average tilting of the mesogens, a different localization or delocalization of the Br^- ions, or even some degree of variability in the local structure involving one or more of those variants that may contribute to the observed weakness of the small-angle reflections; however, this would only change the details of the following discussion, not the overall picture.) The X-ray data for copolymer AB-58 are also consistent with a lamellar structure for the hard phase, but with a thicker layer spacing. With only a single diffraction peak apparent for the hard phase of the other copolymers, its microstructure can only be presumed, and for simplicity, we will presume that lamellar packing is maintained at least locally. We can then identify two distinct ways in which A units might be incorporated into the Bn microstructure, resulting in arrangements that resemble the double-comb bilayer structures of "mixed" and "demixed" side chains considered by Neumann et al.[25] for liquid crystalline random copolymers of two different long side chains.

In the first case, A units are located, or effectively dissolved, within the Bn lamellae (mixed side chains[25]), as illustrated in Figure 6b,c. This causes extension of the alkyl side-chain spacers to accommodate the added volume of the A units while maintaining maximal ionic interactions, thus accounting for a progressive increase in lamellar thickness, d, with A content. At low A content, the partial bilayer structure of the Bn phase can remain intact with the Br tip of the A unit "adsorbed" near the pyridinium sublayer, or the Br tip may insert itself in the pyridinium sublayer as also

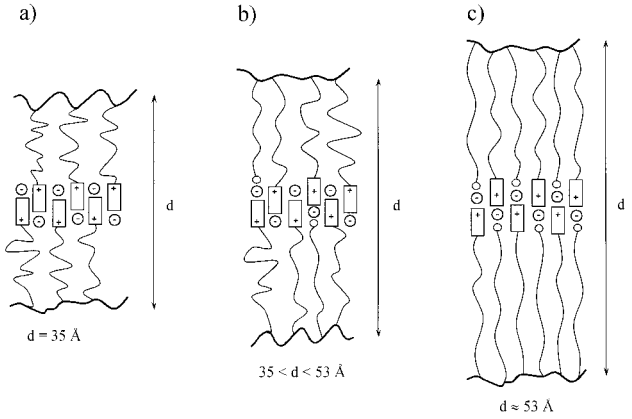

Figure 6. Idealized schematic models of mixed structures showing how A can be accommodated within the Bn microstructure, with corresponding lamellar thicknesses, d, indicated: (a) pure Bn microstructure, (b) low A content, (c) maximal A incorporation.

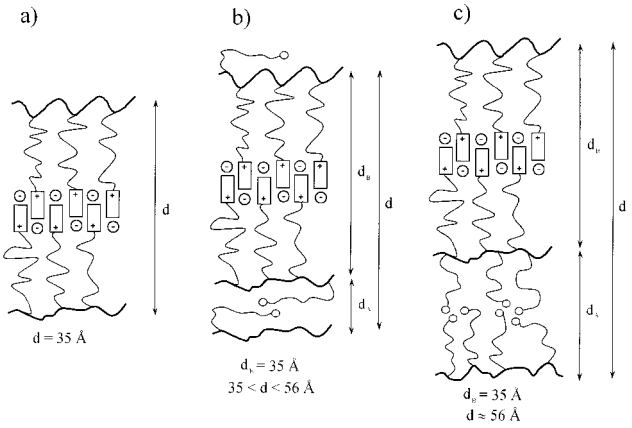

Figure 7. Idealized schematic models of demixed structures, with corresponding lamellar (d) and sublamellar (d_A and d_B for the A and B sublayers, respectively) thicknesses indicated: (a) pure Bn microstructure, (b) low A content, (c) high A content (approximately 50 mol %).

shown (Figure 6b). In the latter case, the interdigitation of the pyridinium groups is decreased, which may be accommodated by appropriate delocalization or relocalization of the positive charge to maintain optimal electrostatic interactions. At high A content, the structure shown in Figure 6c can be envisaged. It allows for maximal incorporation of A units (about 50 mol %) with the B units in efficiently packed lamellae and gives a lamellar thickness estimated to be about 53 Å. This mixed structure is all the more conceivable in that the terminal Br atom of A can be attracted to the ionic sublayer by dipolar forces.

Another way to incorporate A units into the Bn microstructure is by nanophase separation of the A and B units (demixed side chains[25]), such that each lamellae is composed of a B sublayer with unperturbed Bn packing (constant d_B equal to d of Bn) and an A sublayer whose thickness, d_A, varies with A content, as illustrated in Figure 7b,c. At low A content, the A sublayer may be thin (small d_A) to favor uniform coverage of the B sublayers (Figure 7b). This is conceivable given the disordered (noncrystalline) state of the A side chains combined with the lack of rigid mesogen and the relatively weak amphiphilic character of the Br-terminated alkyl chain so that minimal bromine aggregation can be tolerated. With increasing A content,

the A sublayer thickens due to the A alkyl chains becoming increasingly extended in order to accommodate the increasing amount of A. This is shown in Figure 7c for about 50 mol % A, giving a total lamellar thickness of about 56 Å. The latter coincides with the sum of the Bragg spacings of Bn and An (considering the An peak near 4.3°), which possibly represents a maximum lamellar thickness for the demixed structure. However, a greater maximal thickness or an indefinite lamellar thickness is not excluded. It may be added that the arrangement of the A units shown in Figure 7c, although reasonable, is hypothetical.

On the basis of the available data, it is not possible to decide unequivocally between the two structures. Nor are they necessarily mutually exclusive. For example, the copolymer hard phase may be essentially a mixed structure accompanied by some additional thickening due to demixed A; this may account for the estimated maximum lamellar thickness for the mixed structure being somewhat short of the highest *d*'s measured, 58 Å. On the other hand, a basically demixed structure with a certain amount of dissolved A in the B sublayer, or intermediate mixed/demixed structures are also conceivable. The most important result is that the models proposed rationalize the incorporation of a high proportion of A units in the hard phase.

In contrast, essentially no B units are incorporated into the soft-phase (An) microstructure over the entire range of copolymer compositions studied. This is in opposition to what is generally observed in ionomers where a certain proportion of ionic groups or aggregates (multiplets) are generally dispersed within the soft phase.[1] In terms of a possible A-dominated mixed structure, this exclusion can be rationalized by noting the very different shape of the relatively elongated, planar (due to charge delocalization), and rigid DMAP moiety compared to the simple Br sphere. Given that the An phase is itself structured, however imperfectly, it can thus be expected that pyridinium moieties will perturb the local packing of the Br units in the An phase (in contrast to A in the Bn phase), thus disfavoring any A-dominated mixed structure. In terms of a possible demixed structure, the exclusion can be rationalized by considering, first, that when the ionic groups in ionomers are located far from the polymer backbone, as in the present case, the ionic aggregates are generally large because of less steric hindrance to such aggregation.[1,11] This, along with the tendency of the B units to form lamellae and their capacity to incorporate high proportions of A units as described above, would result immediately in a B-dominated microstructure (hard phase) rather than in an A-dominated demixed microstructure (soft phase containing B units) in the regions of ionic aggregation. This is all the more plausible given that there are variable length sequences of A and B in random copolymers: thus, the A units in longer sequences of A in a given polymer chain are the most likely to form the pure soft phase, whereas those in shorter sequences are most susceptible to being incorporated into the hard-phase microstructure.

The thermal behavior is consistent with the proposed models, keeping in mind the different detection limits of the DSC and X-ray methods. First, the increase in T_g of the soft phase for AB-27 and the inability to detect any soft phase by DSC for AB-58, despite its presence in essentially pure form in both copolymers according to X-ray analysis, can reasonably be interpreted as reflecting the simultaneous decrease in the size of the An domains (to below the DSC detection limit for AB-58) and in their mobility due to their interconnectedness with the less mobile ionic hard-phase domains, as the A content decreases. Furthermore, the decrease in the T_g of the hard phase can be attributed, in part, to the incorporation of the A units in either mixed or demixed structures and, in part, to An domains that are too small and rigidified to participate in the DSC soft-phase T_g. The high proportion of A units in the hard phase as calculated from the DSC data (W_A^H) also concords with the models, although, again, part of this proportion must reside in small An domains. It is notable that AB-58 has less than 50 mol % A in its hard phase (its only DSC-detectable phase), and its *d* is also significantly less than the maximum lamellar thickness suggested by the models. On the other hand, the estimated A content in the hard phase of the biphasic copolymers ($y \leq 27$) is greater than 50 mol % according to the DSC analyses, and their *d*'s are correspondingly similar to or greater than what the models suggest for the incorporation of about 50 mol % A.

It is of interest, in this connection, that the Bragg spacings, *d*, obtained for the hard phase from the small-angle X-ray results (Figure 4) and the A content in the hard phase, W_A^H, obtained from the DSC calculations ($1 - W_B^H$, Table 1) can be related, to a first approximation, by the linear relationship

$$d\ (\text{Å}) = 34.1 + 18.8 W_A^H \qquad R(5) = 0.9937 \qquad (8)$$

where *R* is the regression coefficient of the data for the five polymers involved (Bn, for which $W_A^H = 0$, and the copolymers). This relationship neglects any difference in specific volume between the A and B units and does not take into account the different detection limits of DSC and X-ray. Nevertheless, it indicates the coherence of the two sets of data as well as their consistency with the proposed models for the hard phase.

Two final aspects may be discussed briefly. First, it may be noted that the first-order small-angle peak of the Bn pattern in the X-ray profiles can be viewed as the so-called "ionomer peak" generally observed in ionomers.[1] In the EHM model,[17] this peak is considered to represent the average distance of closest approach between neighboring ionic aggregates or multiplets. In our case, with the aggregates considered to be in lamellar domains, the lamellar thickness (or the long period) is simultaneously the effective distance of closest approach between neighboring pyridinium subplanes.

Finally, our system may be contrasted with siloxane dizwitterionic copolymers reported in the literature.[26] These also form lamellar ionic domains, but the lamellar structure is the same throughout the material, consisting of a very thin, zwitterionic and hard, sublayer and a very thick, nonpolar and soft, polysiloxane sublayer that possesses no internal structure. The long period varies from 50 to 400 Å in order of decreasing ion content (studied up to 10 mol % ionic units only). Our system, in the ion content range studied by us, presents a greater level of complexity, where pure An soft-phase domains of unspecified overall geometry but with an internal (possibly lamellar) microstructure coexist with hard-phase lamellar domains that are also of unspecified overall geometry but possess a specific internal microstructure in the form of (lamellar) mixed and/or demixed domains of A and B units.

Conclusions

We have synthesized a series of homologous tail-end, long side-chain statistical comb copolymers, with ion contents ranging between 0 and 100 mol %, by partially quaternizing poly(12-bromododecyl methacrylate) with (dimethylamino)pyridine. They are ionomer-like at lower ion contents, with two DSC-detectable T_g's found up to at least 27 mol %, whereas X-ray analysis indicates a two-phase structure for all the copolymer compositions studied.

The soft-phase microstructure, the same as that of the nonionic homopolymer, appears invariant over the whole range, indicating that ionic units are rejected from this phase. This is in agreement with the constant soft-phase T_g for $F_B < 0.2$, whereas the increase in this T_g for $F_B = 0.27$ and then its disappearance in DSC at higher ion content (F_B/0.58) can be explained by the simultaneous decrease in size of the pure soft phase to below the DSC detection limit and in its mobility due to strong coupling with the surrounding hard phase by interconnecting chains. The rejection of ionic units from the soft phase is attributed to its microstructure, which would be perturbed by the much bulkier ionic unit, as well as to the tendency of decoupled ionic units (as terminal moieties of long side chains) to form large ionic aggregates, which, in the range of ion contents studied, lead directly to the hard-phase microstructure.

In contrast, the long period of the hard phase increases with decreasing ion content, which is attributed to the incorporation of nonionic units in the hard-phase microstructure. This is rationalized by demonstrating that both mixed and demixed layer structures can accommodate up to at least 50 mol % nonionic units within the basic disordered bilayer structure of the ionic homopolymer, resulting in increased lamellar thickness consistent with the X-ray data. The increasing incorporation of nonionic units into the hard phase with increase in copolymer A content concords with the monotonic decrease of the hard-phase T_g, and the large amounts involved are in good agreement with DSC calculations.

Thus, the copolymer series investigated spans materials with ionomer and mesomorphic characteristics by the presence of two phases whose relative proportions vary with ion content, as in classical ionomers. Both phases possess their own (short-range) mesomorphic microstructure that determines the nature of their evolution with copolymer composition. In this context, the SAXS long period that characterizes the lamellar thickness of the hard-phase microstructure can be identified with the so-called "ionomer peak".

Acknowledgment. The financial support of NSERC-Canada (Research Grants Program) and FCAR-Québec (Centres de recherche and Équipes de recherche programs) is gratefully acknowledged. The collaboration was made possible by the FCAR program, Action concertée de soutien à la coopération scientifique internationale, which provided travel grants to P.Y.V. and C.G.B. We also thank Mme Hélène Bellissent for the invaluable help given to P.Y.V. in the syntheses accomplished at ICS and Prof. Josée Brisson of l'Université Laval for her assistance in optimizing the small-angle X-ray setup.

References and Notes

(1) Eisenberg, A.; Kim, J.-S. *Introduction to Ionomers*; John Wiley & Sons: New York, 1998. Schlick, S., Ed. *Ionomers*: *Characterization, Theory and Applications*; CRC Press: Boca Raton, FL, 1996.
(2) McArdle, C. B., Ed. *Side Chain Liquid Crystal Polymers*; Chapman and Hall: New York, 1989. Shibaev, V. P., Lam, L., Eds.; *Liquid Crystalline and Mesomorphic Polymers*; Springer-Verlag: New York, 1994.
(3) Platé, N. A.; Shibaev, V. P. *J. Polym. Sci., Macromol. Rev.* **1974**, *8*, 117.
(4) Köberle, P.; Laschewsky, A. *Macromolecules* **1994**, *27*, 2165.
(5) Vuillaume, P. Y.; Bazuin, C. G.; Galin, J.-C. *Macromolecules* **2000**, *33*, 781.
(6) Köberle, P.; Laschewsky, A.; van den Boogaard, D. *Polymer* **1992**, *33*, 4029.
(7) Zhao, Y.; Lei, H. *Macromolecules* **1994**, *27*, 4525. Lei, H.; Zhao, Y. *Polym. Bull.* **1993**, *31*, 645.
(8) Wiesemann, A.; Zentel, R.; Pakula, T. *Polymer* **1992**, *33*, 5315. Wiesemann, A.; Zentel, R.; Lieser, G. *Acta Polym.* **1995**, *46*, 25.
(9) Masson, P.; Gramain, Ph.; Guillon, D. *Macromol. Chem. Phys.* **1995**, *196*, 3677. Navarro-Rodriguez, D.; Guillon, D.; Skoulios, A.; Frère, Y.; Gramain, Ph. *Makromol. Chem.* **1992**, *193*, 3117.
(10) Lin, C.; Cheng, P.; Blumstein, A. *Mol. Cryst. Liq. Cryst.* **1995**, *258*, 173.
(11) Gauthier, M.; Eisenberg, A. *Macromolecules* **1990**, *23*, 2066. Moore, R. B.; Bittencourt, D.; Gauthier, M.; Williams, C. E.; Eisenberg, A. *Macromolecules* **1991**, *24*, 1376.
(12) Abboud, J. L. M.; Notaris, R.; Bertram, J.; Sola, M. *Prog. Phys. Org. Chem.* **1993**, *19*, 1.
(13) Luca, C.; Avram, E.; Petrariu, I. *J. Macromol. Sci., Pure Appl. Chem.* **1988**, *A25*, 345.
(14) Tsuchida, E.; Irie, S. *J. Polym. Sci., Polym. Chem. Ed.* **1973**, *11*, 789. Luca, C.; Petrariu, I.; Dima, M. *J. Polym. Sci., Polym. Chem. Ed.* **1979**, *17*, 3879. Luca, C.; Avram, E.; Holerca, M. N. *J. Macromol. Sci., Pure Appl. Chem.* **1996**, *A33*, 233.
(15) Platé, N. A.; Litmanovitch, A. D.; Noah, O. V. *Macromolecular Reaction Peculiarities*: *Theory and Experimental Approaches*; Wiley: Chichester, 1995.
(16) Frensdorff, H. K.; Ekiner, O. *J. Polym. Sci.* **1967**, *A2*, 1157.
(17) Eisenberg, A.; Hird, B.; Moore, R. B. *Macromolecules* **1990**, *23*, 4098.
(18) Grassl, B.; Meurer, B.; Scheer, M.; Galin, J. C. *Macromolecules* **1997,** *30*, 236.
(19) Speckhard, T. A.; Hwang, K. K. S.; Yang, C. Z.; Laupan, W. R.; Cooper, S. L. *J. Macromol. Sci., Phys.* **1984**, *B23*, 175.
(20) Bazuin, C. G.; Plante, M.; Varshney, S. K. *Macromolecules* **1997**, *30*, 2618.
(21) Ehrmann, M.; Mathis, A.; Meurer, B.; Scheer, M.; Galin, J. C. *Macromolecules* **1992**, *25*, 2253.
(22) Velankar, S.; Cooper, S. L. *Macromolecules* **1998**, *31*, 9181; **2000**, *33*, 382.
(23) ten Brinke, G.; Karasz, F. E.; Ellis, T. S. *Macromolecules* **1983**, *16*, 244.
(24) Laleg, M.; Camberlin, Y.; Boiteux-Steffan, G.; Seytre, G.; Pascault, J.-P. *J. Macromol. Sci., Phys.* **1984**, *B23*, 233.
(25) Neumann, H. J.; Jarek, M.; Hellmann, G. P. *Macromolecules* **1993**, *26*, 2489.
(26) Graiver, D.; Litt, M.; Baer, E. *J. Polym. Sci., Polym. Chem. Ed.* **1979**, *17*, 3573.

MA001000M